frontiers | Frontiers in Nutrition

TYPE Original Research
PUBLISHED 14 September 2022
DOI 10.3389/fnut.2022.994971

OPEN ACCESS

EDITED BY
Changyang Ma,
Henan University, China

REVIEWED BY
Somanjana Khatua,
Krishnagar Government College, India
Zhenhua Liu,
Henan University, China

*CORRESPONDENCE
Cuiping Feng
ndfcp@163.com

SPECIALTY SECTION
This article was submitted to Nutritional Immunology, a section of the journal Frontiers in Nutrition

RECEIVED 15 July 2022
ACCEPTED 15 August 2022
PUBLISHED 14 September 2022

CITATION
Qiao Z, Zhao Y, Wang M, Cao J, Chang M, Yun S, Cheng Y, Cheng F and Feng C (2022) Effects of *Sparassis latifolia* neutral polysaccharide on immune activity *via* TLR4-mediated MyD88-dependent and independent signaling pathways in RAW264.7 macrophages.
Front. Nutr. 9:994971.
doi: 10.3389/fnut.2022.994971

Effects of *Sparassis latifolia* neutral polysaccharide on immune activity *via* TLR4-mediated MyD88-dependent and independent signaling pathways in RAW264.7 macrophages

Zening Qiao, Yue Zhao, Menghao Wang, Jinling Cao, Mingchang Chang, Shaojun Yun, Yanfen Cheng, Feier Cheng and Cuiping Feng*

College of Food Science and Engineering, Shanxi Agricultural University, Jinzhong, China

Background: *Sparassis latifolia* (*S. latifolia*) is a precious edible fungus with multiple biological activities. To date, no study has been investigated the underlying molecular mechanism of immunoregulation caused by the neutral polysaccharide of *S. latifolia*.

Materials and methods: To investigate immunomodulatory mechanism of *S. latifolia* neutral polysaccharide (SLNP), SLNP was obtained from *S. latifolia* and its structure, immune receptors and regulation mechanism were studied.

Results: *S. latifolia* neutral polysaccharide consisted of arabinose, galactose, glucose, xylose, and mannose with a molar ratio of 6:12:63:10:5. SLNP was a pyran polysaccharide with a relative molecular weight of 3.2×10^5 Da. SLNP promoted the proliferation of RAW264.7, which further induced the secretions of nitric oxide, TNF-α, IL-6, and IFN-β, and upregulated the immune receptor TLR4 expression. Moreover, SLNP increased remarkably the levels of TRAF6, IRF3, JNK, ERK, p38, and p38 mRNA and protein mediated by TLR4.

Conclusion: *S. latifolia* neutral polysaccharide regulated the immune function of RAW264.7 through MyD88-dependent and -independent signaling pathways mediated by TLR4 receptor, which suggests that SLNP is a new immunomodulator.

KEYWORDS

***Sparassis latifolia*, neutral polysaccharide, macrophage RAW264.7, immune activity, toll-like receptor-4, MyD88 signaling pathway**

Introduction

Sparassis latifolia (*S. latifolia*) is a rare edible fungus and is generally called the cauliflower fungus in China owing to its shape. It has been reported that β-glucan content of *S. latifolia* exceeds 40% (1). Previous studies have shown that *S. latifolia* containing β-glucan has a variety of biological activities, such as improving immunity, lowering cholesterol, anti-diabetes, anti-cancer, and anti-inflammation and so on (2, 3). Nowadays, primary interest has been devoted to polysaccharides of *S. latifolia* because of their effectiveness in enhancing immune function (4). *S. latifolia* polysaccharide could enhance the response of hematopoiesis (5). The cyclophosphamide-induced leukemia mice are treated with *S. latifolia* polysaccharides orally, the recovery speed of leukocytes in the organs of the mice is accelerated, and the productions of interferon α (IFN-α), tumor necrosis factor α (TNF-α), and interleukin 6 (IL-6) and other cytokines are significantly increased (6). *S. latifolia* polysaccharides can exert antibacterial effects by inhibiting dysfunction of catabolism and energy metabolism (7). The novel acidic polysaccharides purified from *S. latifolia* in our previous study, with molecular weight (Mw) of approximately 215 Da–393 kDa, has a certain reducing ability and can scavenge effectively DPPH, -OH, O_2^- free radicals and promote the proliferation of RAW264.7 macrophages (8).

As crucial immunocytes derived from differentiation of blood monocytes, macrophages are important components of the immune system and play vital roles in the innate immune response and adaptive immunity, which are one of the first lines of defense against the source of infections (9, 10). Activated macrophages can enhance the organism's defense by phagocytosis and release of inflammatory mediators such as NO and pro-inflammatory cytokines including TNF-α and IL-6 (11). RAW264.7 is a macrophage/monocyte-like cell line used to investigate interactions of polysaccharides and macrophages (12–14).

Toll-like receptors (TLRs) are related to the activation of macrophages. TLR4 is a key pattern recognition receptor that recognizes pathogen-associated molecular patterns and submits signals to cytoplasm to activate transcription factors thus produce proinflammatory cytokines (15, 16). Recently, some studies have shown that many natural polysaccharides exert immunomodulatory functions by acting on TLR4 on the surface of macrophages, such as *Dendrobium officinale* polysaccharide and *Poria Cocos* polysaccharide exerted an immune-potentiating effect through TLR4 (17, 18). Once being recognized, TLR4 can trigger downstream signaling pathways and then medicate the activation of mitogen-activated protein kinase (MAPK), which is a critical signaling pathway and plays a crucial role in the immune system (19, 20). *S. latifolia* polysaccharides can act through the TLR4 receptor to enable the downstream MAPK signaling pathway to activate dendritic cells (21). *Platycodon grandiflorum* (PG) polysaccharides induce dendritic cell maturation by activating MAPK and NF-κB signaling downstream of TLR4 (22). TLR4 is a membrane receptor of *Pueraria lobata* polysaccharide (PLP), which induces functional maturation of dendritic cells through TLR4 signaling (23). As such, TLR4 and downstream signaling pathways can be the targets of polysaccharides. Although the immunomodulatory effect of acidic polysaccharides of *S. latifolia* has been reported in previous studies, whether the neutral polysaccharide of *S. latifolia* (SLNP) regulates the immune activity *via* TLR4-mediated downstream signaling pathways and the underlying mechanism is still unclear. Hence, it is vital to investigate the underlying molecular mechanism of immunoregulation caused by SLNP.

In this study, to investigate the immunomodulatory effect of SLNP and the underlying mechanism, we first extracted and purified a neutral polysaccharide from the *S. latifolia* fruiting body, the structure of which was characterized by a combination of chemical and instrumental analysis of monosaccharide composition, fourier transform infrared spectra (FT-IR), high performance liquid gel permeation chromatography (HPGPC), and nuclear magnetic resonance (NMR). In addition, we assessed the immune potential of SLNP in RAW264.7 macrophages, and investigated the relationship between the immune activity of SLNP and TLR4-mediated myD88 dependent and independent signaling pathways.

Materials and methods

Materials

Dry *S. latifolia* fruiting body were provided by Taihe edible fungus cultivation base in Shanxi Province of China, which were dried treatment in an oven at 35°C. The dry *S. latifolia* fruiting body were sliced into pieces, sieved into 200 mesh powder, and stored sealed at 4°C.

Macroporous resin HZ-830, DEAE-52 cellulose powder, 3-(4,5-dimethylthiazolyl-2)-2,5-diphenyl tetrazolium bromide (MTT), penicillin-streptomycin, dimethyl sulfoxide (DMSO), trypsin (Parenzyme), ethidium bromide, phenylmethyl sulfonyl fluoride (PMSF), and polyvinylidene difluoride (PVDF) were

Abbreviations: SLNP, *Sparassis latifolia* neutral polysaccharide; DMSO, dimethyl sulfoxide; PMSF, phenylmethyl sulfonyl fluoride; PVDF, polyvinylidene difluoride; Glc, D-glucose; Man, D-mannose; Xyl, D-xylose; Gal, D-galactose; Ara, L-arabinose; Fru, D-fructose; LPS, Lipopolysaccharide; IC, Ion chromatography; FT-IR, Fourier transform infrared spectroscopy; FBS, fetal bovine serum; MTT, [3-(4, 5-dimethylthiazol-2-yl)-2,5-diphenyl tetrazolium bromide]; MW, molecular weights; HPGPC, high performance gel permeation chromatography; PMSF, phenylmethylsulfonyl fluoride; ECL, enhanced chemiluminescence.

purchased from Solarbio Science & Technology Co. (Beijing, China). Dextran standard products of T-3, T-10, T-40, and T-70 were obtained from BioDee Biotechnology Co. (Beijing, China). Monosaccharide standards of D-glucose (Glc), D-mannose (Man), D-xylose (Xyl), D-galactose (Gal), L-arabinose (Ara), and D-fructose (Fru), and Lipopolysaccharide (LPS) were purchased from Sigma (St. Louis, MO, United States).

RAW264.7 cells were purchased from Cell Resource Center, Shanghai Institutes for Biological Sciences, Chinese Academy of Sciences (Shanghai, China). Fetal bovine serum (FBS) and Dulbecco's modified eagle medium (DMEM) high glucose medium were obtained from Zhejiang Tianhang Biotechnology Co. (Hangzhou, China) and HyClone (Utah, United States). The Micro NO Content Assay Kit, SDS-PAGE gel configuration kit, BCA protein concentration determination kit, high-sensitivity chemiluminescence detection kit, and RIPA cell lysate were obtained from Beyotime Institute of Biotechnology (Shanghai, China). Assay kits for TNF-α, IL-6, and IFN-β were purchased from Shanghai Westang Biotechnology Co. (Shanghai, China). RNAiso Plus, SYBR® Premix Ex TaqTM II (Tli RNaseH Plus), PrimeScriPt^{TM} RT Master Mix (Perfect Real Time) were purchased from Takara Biomedical Technology Co., Ltd. (Dalian, China). The primary antibodies of TLR4 (bs-1021R), IRF3 (bs-2993R), JNK (bs-2592R), p-JNK (bs-1640R), ERK (bs-2637R), p38 (bs-0637R), and β-actin, and the secondary antibodies of HRP-labeled goat anti-mouse IgG (bs-0295G) were purchased from Bioss Biotechnology Co. (Beijing, China). And the primary antibodies of tumor necrosis factor receptor-related kinase 6 (TRAF6) (66498-1-lg) were purchased from Proteintech Group, Inc. (Wuhan, China).

Extraction and purification of *Sparassis latifolia* neutral polysaccharide

The dry powder of SLNP was mixed with ultrapure water at a ratio of 1:40 (g:mL), and hydrolyzed at 75°C for 2 h. After being centrifuged at 4500 rpm for 10 min, the supernatant was concentrated, added ethanol at a ratio of 1:3 (mL:mL), and kept at 4°C for 12 h. The precipitate was collected by centrifugation at 5000 rpm for 5 min, and washed with acetone and ether for several times, dissolved in ultrapure water at 45°C for 8 h. Afterward, the supernatant was added Sevag solvent (Chloroform: N-butanol = 4:1), stirred by magnetic stirrer for 20 min, and centrifuged at 5000 rpm for 5 min. Next, the obtained supernatant was preliminarily decolorized and removed impurities by HZ-830 Macroporous Adsorption Resin to obtain crude polysaccharides. Then the 10 mg/mL crude polysaccharides were eluted in a DEAE-52 cellulose chromatography column (2.6 cm × 30 cm) with ultrapure water at a flow rate of 1 mL/min. The obtained polysaccharides were measured the content by the phenol sulfuric acid assay. Finally, the purified neutral polysaccharides were collected, dialyzed, and lyophilized.

Molecular weight

The Mw of SLNP was evaluated by HPGPC (Agilent, United States) with a final concentration of 0.5 mg/mL and the injection volume of 20 μL using a detector differential refractive index detector and a TSK-GEL-4000 PWXL column (Agilent, United States) eluting with ultrapure water. The column temperature was 40°C, and the flow rate was 0.6 mL/min. T-dextran standards with different molecular masses were used for injection under the same conditions and the standard curve was drawn with the peak time as the abscissa and the relative Mw as the ordinate.

Monosaccharide composition analysis

Twenty mg of SLNP was mixed with 4 mL of trifluoroacetic acid in a sealed test tube and was put into an oven to hydrolyze at 120°C for 6 h. Then the hydrolysate was added methanol to evaporate trifluoroacetic acid completely and dissolved in 1 mL of distilled water. Afterward, the obtained solution was diluted 10 times to measure the monosaccharide composition by ion chromatography (IC) with Dionex Carbopac PA10 column (250 mm × 4 mm) and Dionex pulsed amperometric detector (California, United States) with Au electrode. The detection conditions were as follows: the column temperature was 30°C, the injection volume was 25 μL, the flow rate was 0.45 mL/min, and elution mode was 10% 200 mmol/L NaOH and 90% ultrapure water. Glucose, fructose, mannose, xylose, galactose, and arabinose were selected as standard monosaccharide.

Fourier transform infrared spectra analysis

The functional chemistry of SLNP (2 mg in KBr pellets) was detected with a Bruker Tensor 27 IR instrument (Karlsruhe, German) at a frequency range of 400–4000 cm^{-1}.

Nuclear magnetic resonance spectroscopy

Sparassis latifolia neutral polysaccharide was treated with deuterium (D_2O, 99.9%) and lyophilized with D_2O for three times to exchange protons. Afterward, SLNP was placed in a 5 mm NMR tube and dissolved in 0.5 mL of D_2O. NMR-spectra

was recorded with a Brucker AVANCE III 850 MHz NMR (Karlsruhe, Germany). The analysis included a 1D spectrogram (^{1}H, ^{13}C).

Cell culture

The RAW264.7 macrophages were cultured in DMEM high glucose medium containing 10% fetal bovine serum in a 5% CO_2 incubator at 37°C. Then the cells at the logarithmic growth phase and under stable growth conditions were selected for further experiments.

Cell viability assay

The effects of SLNP on the viability of RAW264.7 cells were measured by MTT method. The RAW 264.7 macrophages were planted into 96-well plates at a density of 1×10^4 cells per well and cultured overnight in a CO_2 cell incubator. Next the cells were cultured with 100 μL of SLNP solution with 12 different concentrations between 1.95 μg/mL and 4000 μg/mL for 24 h, respectively, during which LPS (1 μg/mL) was used as a positive control group, and the culture medium was used as a negative control group. There were 6 replicates in each group. After that, cells in each well were added 20 μL MTT solution to continuously incubate in dark for 4 h. After discarding MTT and adding 150 μL of Dimethyl sulfoxide (DMSO) in each well, the cells were gently shaken on the shaker for 15 min and the cell viability was determined with a SpectraMax i3X microplate reader (Sunnyvale, United States) at 490 nm.

Assay for NO and cytokine secretion

The RAW264.7 cells (2.5×10^5 cells/well) under good growth conditions were seeded in 24-well plates and cultured overnight, and the old medium was discarded after adherent. Then the cells were treated with various concentrations of SLNP (62.5, 125, 250, 500 μg/mL), LPS (1 μg/mL), and the medium for 24 h. There were 4 replicates in each group. Next the supernatants in each well were collected and centrifuged to determine the levels of NO and IL-6, TNF-α, IFN-β by Micro NO Content Assay Kit and the corresponding ELISA kits.

To further study the effects of TLR4 antibody on the secretion of NO and cytokines, the RAW264.7 cells (2.5×10^5 cells/well) in each well were treated with 20 μg/mL of TLR4 antibody for 1 h. Afterward, the cells were treated with 250 μg/mL of SLNP, 1 μg/mL of LPS, and the medium for 24 h. Each group had 4 replicates. After incubation, the supernatants were collected to measure the concentrations of NO and cytokines of IL-6, TNF-α, IFN-β by Micro NO Content Assay Kit and the corresponding ELISA kits.

Quantitative analysis of cytokine mRNA expression

The RAW264.7 cells were planted into 6-well plates at a density of 2×10^6 cells per well for 12 h. After discarding the old medium, cells were incubated with 125, 250, 500 μg/mL of SLNP, 1 μg/mL of LPS, and new medium for another 24 h, respectively. Total RNA was extracted from RAW264.7 cells using the RNAiso Plus according to the manufacturer's protocols. After that, the purity and content of RNA were measured by Nanodrop 2000c (Thermo Fisher, Delaware, United States). Next, cDNA was synthesized from the total RNA with the PrimeScript® RT reagent Kit. Afterward, the mRNA expression levels of *TLR4*, *TRAF6*, *IRF3*, *JNK*, *ERK*, *p38*, and β-*actin* in RAW264.7 macrophages were detected by real-time fluorescent quantitative polymerase chain reaction (qPCR) under the following conditions: 95°C for 90 s, 40 cycles of 95°C for 5 s, 60°C for 30 s, 72°C for 30 s, 95°C for 15 s, 60°C for 1 min, and 95°C for 15 s. The levels of the target genes were calculated according to $2^{-\Delta\Delta Ct}$ method with the β-actin gene as the internal reference. The primers used for qPCR were listed in **Table 1**.

Western blot analysis

After treating with different concentrations of SLNP (125, 250, and 500 μg/mL), 1 μg/mL of LPS and new medium for 24 h, the RAW264.7 cells in each well were added 150 μL of RIPA cell lysate containing PMSF and protein phosphatase inhibitor to lyse for 30 min. After centrifugation at 12,000 r/min for 15 min, the supernatants were collected and stored at −80°C for further use. Afterward, the total protein was quantified using the BCA method, subjected to SDS-PAGE, and transferred onto PVDF membranes. Next, the PVDF membranes were blocked with 5% non-fat milk at room temperature for 2 h, added the specific primary antibody of TLR4 (diluted 1:500), β-actin (1:1000), IRF3 (1:1000), JNK (1:1000), ERK (1:1000), p38 (1:1000), P-JNK (1:1000), and TRAF6 (1:1000), respectively, and shaken overnight at 4°C. After being rinsed 3 times with TBST, the PVDF membrane was added HRP-labeled goat anti-mouse IgG (diluted 1:3,000) and shaken at room temperature for 2 h. After the PVDF membrane was washed with TBST, the antibody-specific protein was observed in a fluorescence imager using eECL kit.

Statistical analysis

The results were expressed as the mean ± standard error (SE). Graphpad Prism 5.0 software was used for one-way analysis of variance followed by Duncan's multiple comparisons.

10.3389/fnut.2022.994971

TABLE 1 Primers used for qPCR.

No.	Genes	Primers (5′- > 3′)	Primer location (start)	Product size (bp)	Genbank No.
1	β-actin	AGCCATGTACGTAGCCATCC CTCTCAGCTGTGGTGGTGAA	1063 1145	83	NM_007393.3
2	TLR4	AATCTGGTGGCTGTGGAG CCCTGAAAGGCTTGGTCT	1536 1766	147	NM_021297.2
3	TRAF6	AGGGCTACGATGTGGAGTT TTTACCGTCAGGGAAAGAAT	162 396	235	NM_009424.3
4	IRF3	CGCTACACTCTGTGGTTCTG GATAGGCTGGCTGTTGGA	1000 1179	180	NM_016849.4
5	JNK	ATTGAACAGCTCGGAACAAC GAGTCAGCTGGGAAAAGCAC	984 1123	140	NM_013693.2
6	ERK	TGACCTCAAGCCTTCCAACC ATCTGGATCTGCAACACGGG	683 770	88	NM_011949.3
7	p38	TCACGCCAAAAGGACCTACC ATTCCTCCAGTGACCTTGCG	632 738	107	NM_001168514.1

$P < 0.05$ was regarded as statistically significant and $P < 0.01$ was considered to indicate a statistically highly significant.

Results

Isolation and purification of *Sparassis latifolia* neutral polysaccharide

After the crude polysaccharides were separated by a DEAE-52 cellulose column, the elution curve was a single and symmetrical peak (**Figure 1**). Next, the eluate was collected, concentrated, dialyzed, and freeze-dried to obtain light yellow neutral polysaccharides. Then the homogeneous SLNP were obtained after being collected and frozen-drying. The HPGPC of SLNP (**Figure 2**) showed that this fraction had a single and symmetrical peak and the relative Mw was 3.2×10^5 Da.

Preliminary structural characterization of *Sparassis latifolia* neutral polysaccharide

The IC technology was used to determine the monosaccharide composition of SLNP. As shown in **Figure 3**, SLNP was mainly composed of arabinose, galactose, glucose, xylose and mannose with molar ratio of 6:12:63:10:5, respectively. Galacturonic acid and glucuronic acid were not detected, which indicated that SLNP was a neutral polysaccharide (24).

Fourier transform infrared spectroscopy was used to analyze the functional group structure of the SLNP. As shown in **Figure 4**, the absorption peak at 3406 cm^{-1} was caused by the stretching vibration of the hydrangea polysaccharide molecule -OH, the absorption peak in the range of 2780–2968 cm^{-1} was caused by the stretching vibration of C-H in the polysaccharide structure (25, 26), the absorption peak at 1631 cm^{-1} was the flexural vibration absorption peak of -OH, and the absorption peak near 1367 cm^{-1} was the flexural vibration absorption peak of C-H (27, 28). The absorption peaks at 1154–1019 cm^{-1} were the absorption peaks caused by the stretching vibration of the C-O-C structure and the C-O-H variable-angle vibration on the polysaccharide ring of *S. latifolia*, 1078 and 1019 cm^{-1} were the characteristic absorption of the pyran ring (29). There was the characteristic absorption peak of C-H variable angle vibration of α-type glycosidic bond near 840 cm^{-1}, and the absorption peak near 890 cm^{-1} was the characteristic absorption peak of C-H variable angle vibration of β-type glycosidic bond, indicating the existence of a pyranose ring connected by α-glycosidic bond and β-glycosidic bond (30). In addition, no absorption peak was

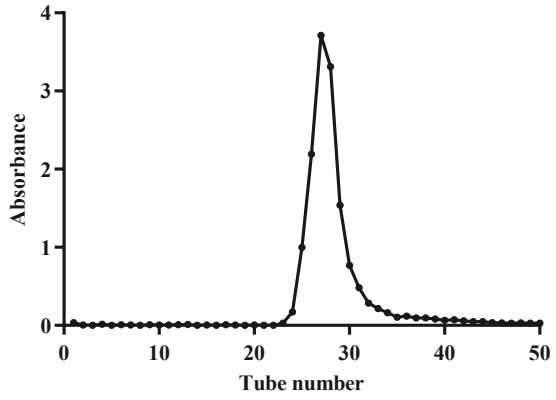

FIGURE 1
Elution curve of crude polysaccharide from *Sparassis latifolia* on DEAE-52 cellulose column.

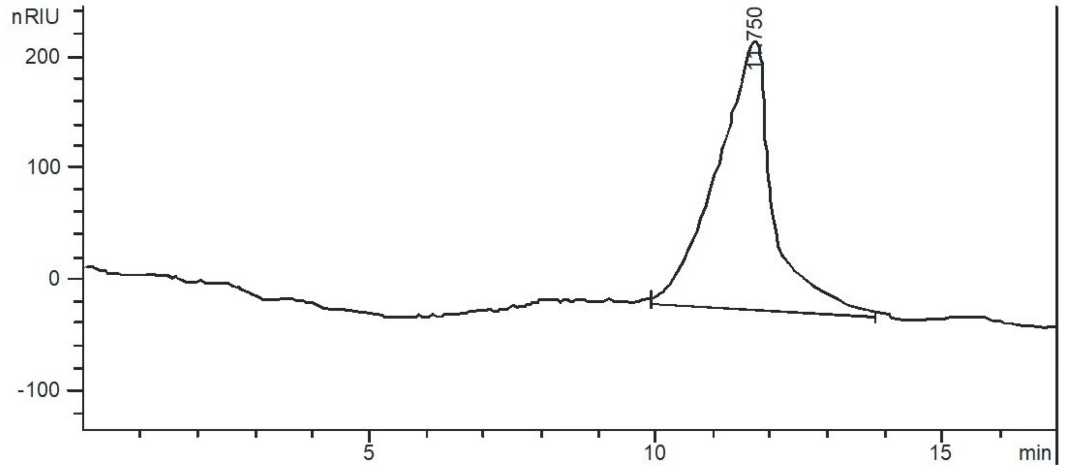

FIGURE 2
High performance gel permeation chromatogram (HPGPC) of *Sparassis latifolia* neutral polysaccharides SLNP.

found near 1730 cm^{-1}, indicating that there is no uronic acid in SLNP (31).

Nuclear magnetic resonance was used to analyze the glycosidic bond configuration of the SLNP. As shown in **Figures 5A,B**, in the ^{1}H-NMR spectrum, the chemical shift at 3.5–4.5 ppm was the proton peak of the sugar ring carbon, and there was an anomeric proton signal absorption peak in the range of 4.5–5.5 ppm. Specifically, the chemical shift of 5.0–5.5 ppm indicates that the polysaccharide is mainly in the configuration, and the weak peak at 4.5–4.6 ppm indicates that the polysaccharide structure has a small amount of β configuration. In the anomeric carbon region of the ^{13}C-NMR spectrum, the two absorption peaks of 98.6 and 100.8 ppm were α-type end group carbon signals, and the absorption peaks of 102.3, 102.7, and 102.9 ppm were β-type. The end-group carbon signal, of which the absorption peak signal at 100.8 ppm was stronger, and the signal at 98.6, 102.3, 102.7, and 102.9 ppm were relatively weak, indicating that SLNP is mainly composed of five monosaccharide residues. Consistent with the results of monosaccharide composition, the main chain might consist of one α-pyranose residue, one α-type sugar residue and three β-type sugar residues to form the side chain. The chemical shifts of 70.3–78.5 ppm were assigned to the unsubstituted C_2-C_5 structure on the sugar ring.

Effects of *Sparassis latifolia* neutral polysaccharide on cell viability of RAW264.7 cells

The RAW264.7 macrophages were treated with different concentration of SLNP for 24 h to determine the cell viability by MTT assay. As shown in **Figure 6**, the proliferation ability of RAW264.7 cells were increased first and then decreased with the increase of SLNP concentration. The proliferation ability was significantly up-regulated after treated with SLNP (7.8125–1000 μg/mL) compared to the control group ($P < 0.05$). Moreover, 250 μg/mL of SLNP had the strongest ability to promote the proliferation of RAW264.7 cells and the upregulation rates were 103.84%. However, after SLNP concentration exceeded 250 μg/mL, the proliferation activity of RAW264.7 cells gradually decreased, and when the concentration was 4,000 μg/mL, SLNP strongly inhibited the proliferation activity of RAW264.7 cells with the inhibition rate of 34.54%.

Effects of *Sparassis latifolia* neutral polysaccharide on production of NO and cytokines in RAW264.7 cells

Activated macrophages can secrete a series of chemokines and cytokines, which play important roles in activating adaptive immune responses and regulating other immune responses (32). ELISA was used to detect the production of NO, IL-6, TNF-α, and IFN-β. Compared with the control group, different concentrations of SLNP up-regulated significantly the levels of NO (**Figure 7A**), IL-6 (**Figure 7B**), TNF-α (**Figure 7C**), and IFN-β (**Figure 7D**) in RWA 264.7 macrophages ($P < 0.01$), of which 250 μg/mL of SLNP had the strongest promotion ability and the upregulation rates were 477.98, 375.45, 721.52, and 260.88%, respectively. Meanwhile, LPS could promote remarkably RWA 264.7 macrophages to produce NO, IL-6, TNF-α, and IFN-β ($P < 0.01$). Above results indicate that SLNP might display immune enhancing activity by inducing the production of NO and cytokines in RAW264.7 cells.

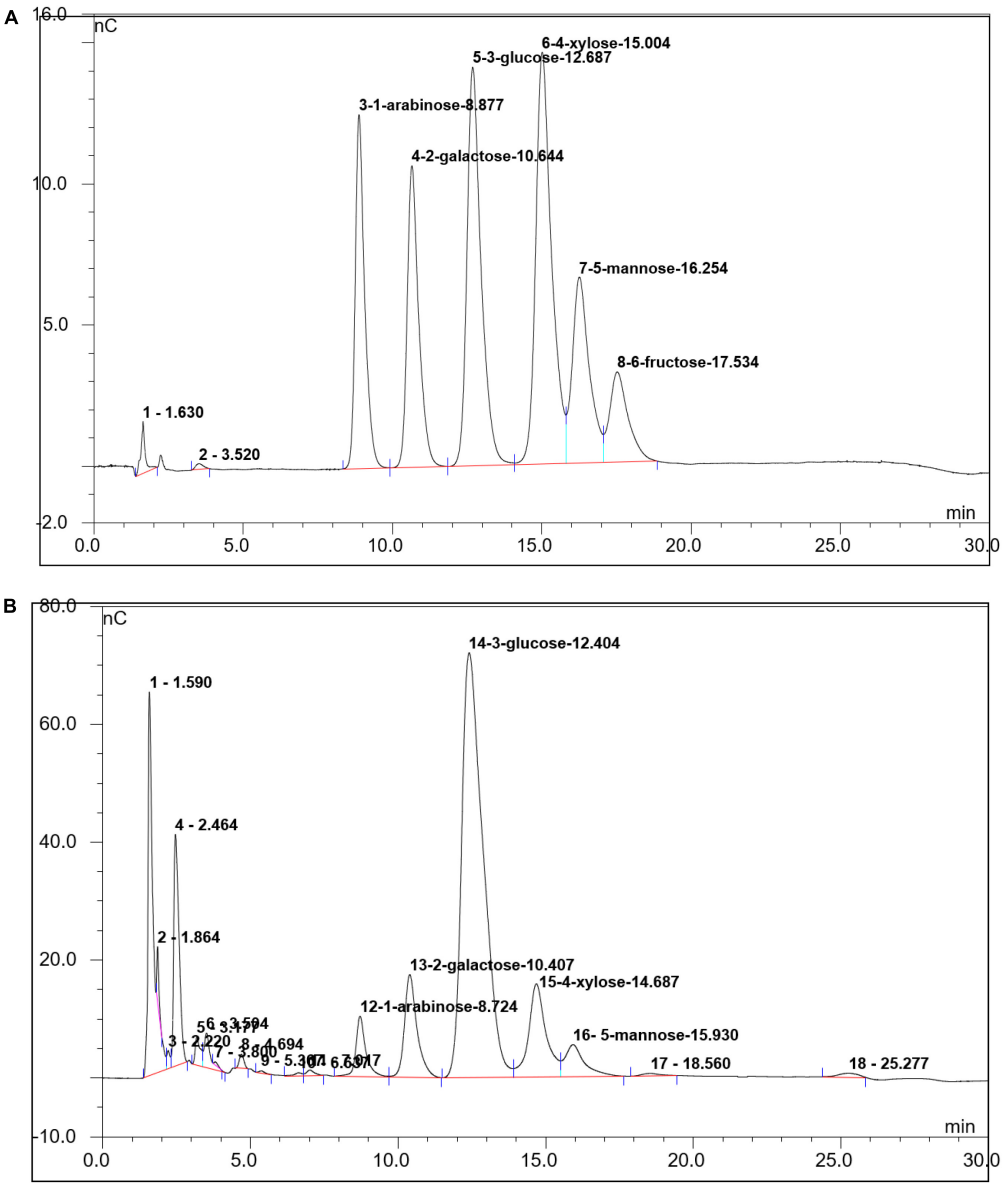

FIGURE 3
Ion chromatogram of *Sparassis latifolia* neutral polysaccharides SLNP. **(A)** Standard Sample; **(B)** SLNP.

Participation of TLR4 in *Sparassis latifolia* neutral polysaccharide-induced macrophages activation

To verify whether TLR4 has participated in SLNP-induced macrophages activation, we investigated the expression of TLR4 mRNA and protein, and the effects of TLR4 antibody on the secretion of NO and cytokines induced by SLNP. The results showed that compared with the control group, the expression levels of TLR4 mRNA (Figure 8A) and protein (Figure 9B) in macrophages were significantly elevated after treatment with different doses of SLNP and 1 μg/mL of LPS ($P < 0.01$). And treatment with 500 μg/mL SLNP increased markedly TLR4 mRNA and protein levels by 52.33 and 96.82%, respectively, implying that TLR4 is an immune recognition receptor in which SLNP plays an immunomodulatory role. However, blocking TLR4 signaling with the specific TLR4 antibody reversed the elevation of NO and cytokines in SLNP-induced RAW264.7 macrophages. As shown in Figure 10, the levels of NO (Figure 10A), IL-6 (Figure 10B), TNF-α (Figure 10C), and IFN-β (Figure 10D) were remarkably increased in macrophages RAW264.7 treated with 250 μg/mL

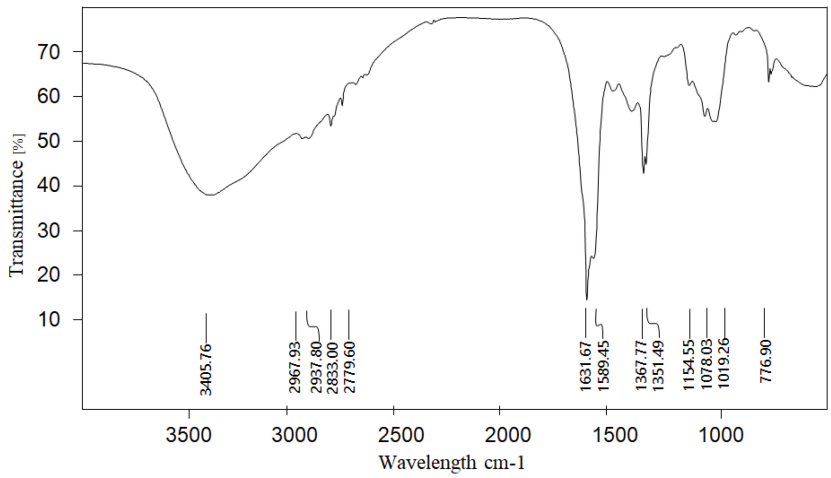

FIGURE 4
Fourier infrared spectrum of *Sparassis latifolia* neutral polysaccharides SLNP.

of SLNP or LPS compared with the control group ($P < 0.01$). However, the TLR4 antibody decreased significantly the levels of NO (Figure 10A), IL-6 (Figure 10B), TNF-α (Figure 10C), and IFN-β (Figure 10D) by 68.87, 68.45, 75.38, and 47.25% compared with 250 μg/mL of SLNP group. The similar trends were found in RAW264.7 cells induced by 1 μg/mL of LPS. In short, these results illustrate that TLR4 participates in SLNP-induced macrophage activation.

Sparassis latifolia neutral polysaccharide activated MyD88-dependent signaling pathway in RAW264.7 cells

In order to explore whether the SLNP-induced up-regulation of TLR4 caused the activation of MAPK signaling pathway, the cells were treated with different concentrations of SLNP, and the mRNA levels of *TRAF6*, *JNK*, *ERK*, and *p38* were measured by qPCR. Meanwhile, to further clarify the mechanism by which SLNP activates the MyD88-dependent pathway, the total levels of TRAF6 and phosphorylation levels of JNK, ERK and p38 were measured by Western Blot (Figure 9A).

As shown in Figure 8, different concentrations of SLNP significantly up-regulated the mRNA levels of *TRAF6* (Figure 8B), *JNK* (Figure 8C), *ERK* (Figure 8D), and *p38* (Figure 8E) compared with the control group ($P < 0.05$). Treatment with 250 μg/mL of SLNP elevated remarkably these indexes by 72.70, 86.54, 82.77, and 56.98%, respectively. The similar trends were found in the protein levels of TRAF6 (Figure 9C), JNK (Figures 9D,E), ERK (Figures 9F,G) and p38 (Figures 9H,I). Compared with the control group, the relative protein levels of TRAF6 (Figure 9C), JNK (Figures 9D,E), ERK (Figures 9E,G) and p38 (Figures 9H,I) in RAW264.7 cells were significantly up-regulated in 250 μg/mL of SLNP group, with the up-regulation rate of 115.13, 147.66, 131.21, and 214.01%. These results suggest that SLNP exerts the immunomodulatory effects by activating MyD88-dependent pathway and the downstream MAPK signaling pathway.

Sparassis latifolia neutral polysaccharide activated MyD88-independent signaling pathway in RAW264.7 cells

TLR4 initiates MyD88-independent signaling pathways which increase the expression of IRF3 resulting in the expression of IFN-β (33). As shown in Figure 8F, after being incubated with SLNP, the expression of *IRF3* mRNA in RAW264.7 cells was increased significantly compared with the control group. The expression of IRF3 protein also showed an increasing trend after treated with SLNP (Figure 9J). Treatment with 500 μg/mL of SLNP increased remarkably the levels of IRF3 mRNA and protein by 28.13 and 18.00% in the RAW264.7 cells, respectively. These results indicate that SLNP activates the MyD88-independent signaling pathway.

Discussion

The fungal polysaccharides have long been believed to possess benign immunoregulatory effects with low toxicity.

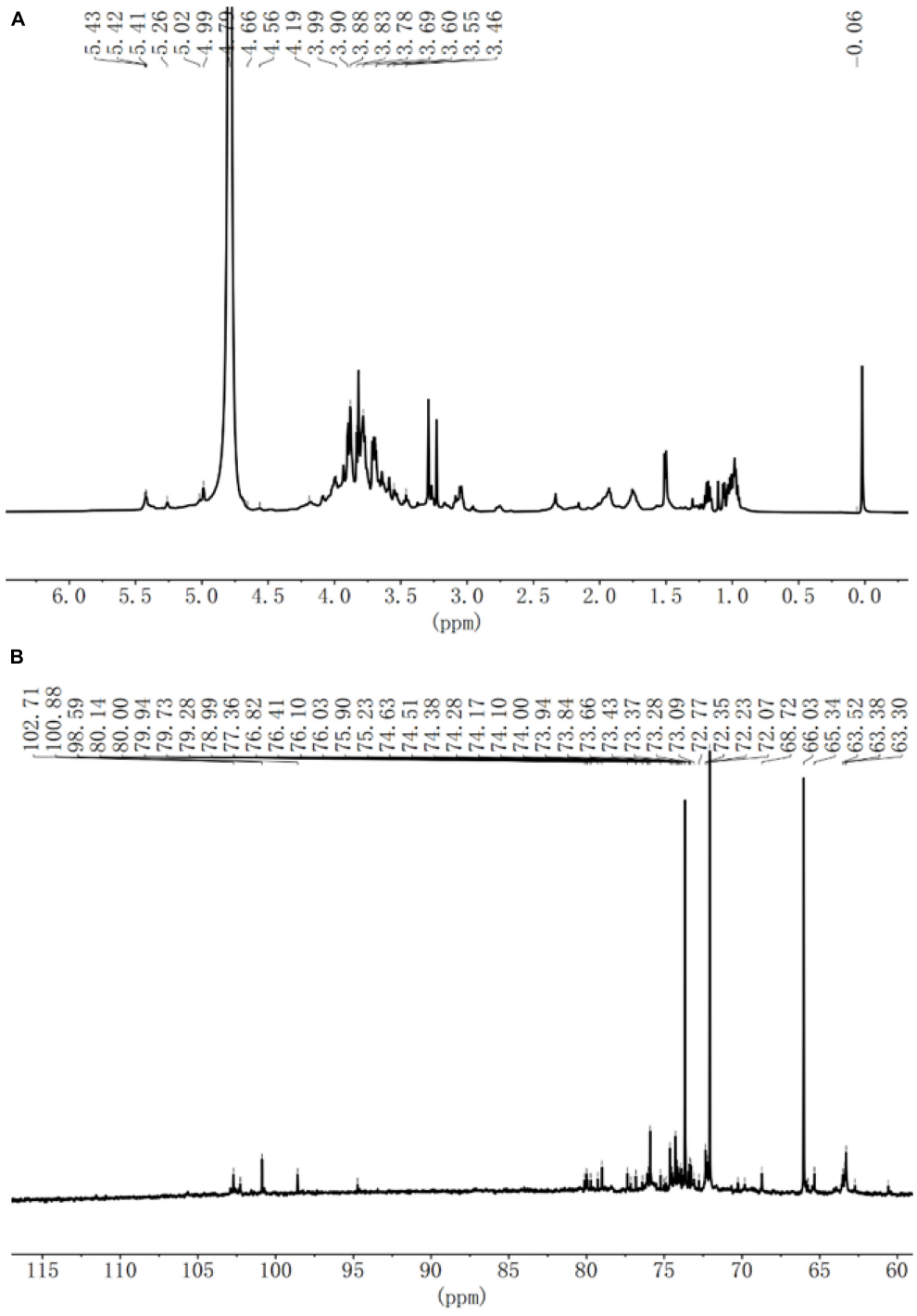

FIGURE 5
(A) 1H NMR spectra of *Sparassis latifolia* neutral polysaccharides SLNP. **(B)** (C)C^{13} NMR spectra of SLNP.

Furthermore, they are considered potent immunomodulatory agents since they activate both innate and adaptive immune responses (34). In addition, polysaccharides can stimulate the secretion of immune factors while activating innate immunity (35, 36). The immunological activity of polysaccharide is strongly associated with its structure, such as Mw, monosaccharide composition and glycosidic bonds (37–39). In this study, a homogeneous polysaccharide with immunological activity was isolated and purified from *S. latifolia* with the relative Mw of 3.2 Da × 10^5 Da. Moreover, previous

10.3389/fnut.2022.994971

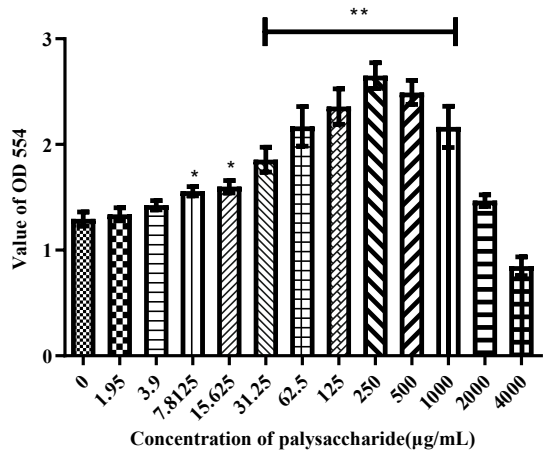

FIGURE 6
Effects of *Sparassis latifolia* neutral polysaccharides SLNP on RAW 264.7 macrophage viabilities. *$p < 0.05$, **$p < 0.01$ vs. control group.

reports have demonstrated that polysaccharides containing galactose, glucose, arabinose and mannose might have tight association with the immunomodulatory activity (40). Similar results were obtained in our study which found that SLNP consisted of arabinose, galactose, glucose, xylose and mannose at the molar ratio of 6:12:63:10:5, respectively. The high proportion of galactose and glucose in SLNP exert a strong immune activity. The FT-IR demonstrated that SLNP had strong absorption peaks near 3400, 2900, and 1600 cm^{-1}, indicating that SLNP has the characteristic functional group structure of polysaccharides (41, 42). In addition, the single symmetrical peak presented by the main peak of SLNP indicates that it is a homogeneous polysaccharide. In summary, the immunomodulatory effect of SLNP is tightly related with its structure. However, the structure of SLNP is not fully clarified. Further study will be conducted to explore its structure deeply.

Macrophages are the main components of the mononuclear phagocyte system, which can not only initiate innate immune response, but also participate in cellular immune responses. The activated macrophages can phagocytose pathogenic microorganisms, process and present antigens, and simultaneously synthesize and secrete chemokines and cytokines to enhance the body's immune defense capabilities (43–45). A great deal of natural polysaccharides can produce an immune effect primarily *via* macrophages (46, 47). *Morchella sextelata* polysaccharides with a concentration of 50–400 μg/mL

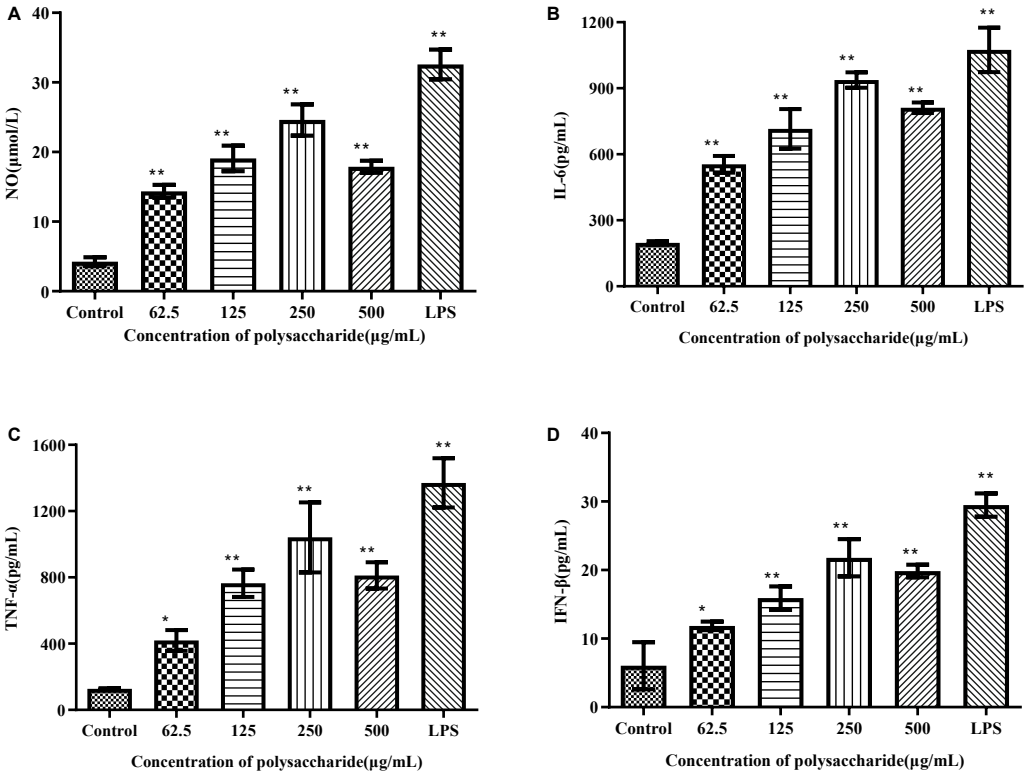

FIGURE 7
Effects of SLNP on NO **(A)**, IL-6 **(B)**, TNF-α **(C)**, IFN-β **(D)** production in RAW264.7 macrophage. Compared with blank control group, *$p < 0.05$,**$p < 0.01$; Compared with LPS control group, $^{\Delta}p < 0.05$, $^{\Delta\Delta}p < 0.01$.

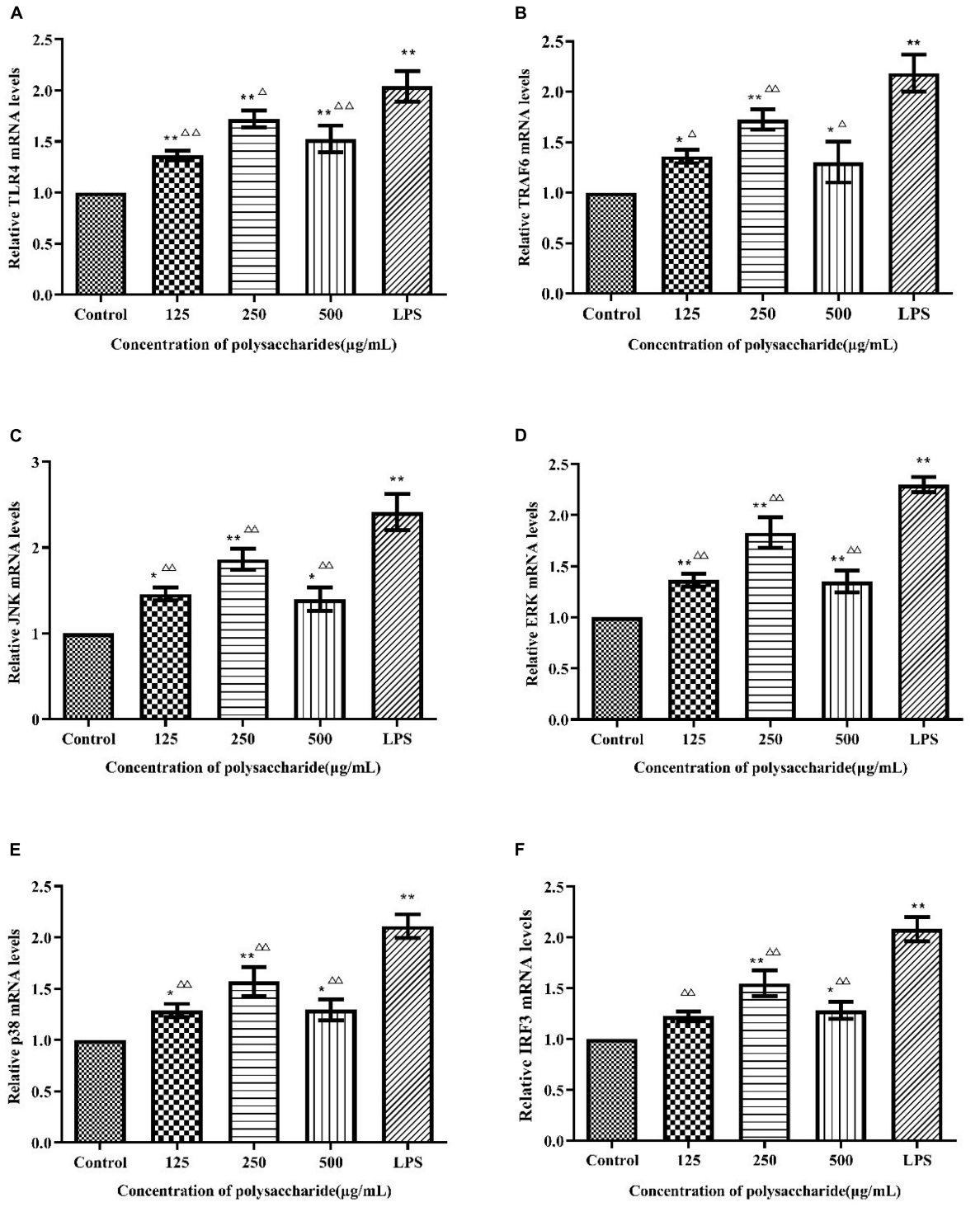

FIGURE 8
Effects of *Sparassis latifolia* neutral polysaccharides SLNP on mRNA expression of TLR4 **(A)**, TRAF6 **(B)**, JNK **(C)**, ERK **(D)**, p38 **(E)**, and IRF3 **(F)** on RAW264.7 macrophage. Compared with blank control group, $^{*}p < 0.05$, $^{**}p < 0.01$; Compared with LPS control group, $^{\Delta}p < 0.05$, $^{\Delta\Delta}p < 0.01$.

can promote the proliferation of RAW264.7 cells (48). Polysaccharides isolated from *Sarcodon aspratus* are not toxic to RAW264.7 cells within a certain concentration range of 25–100 μg/mL (49). *Russula alutacea Fr.* polysaccharides exhibit the capacity to promote the proliferation of RAW264.7 cells at 25–200 μg/mL, and don't show cytotoxicity even

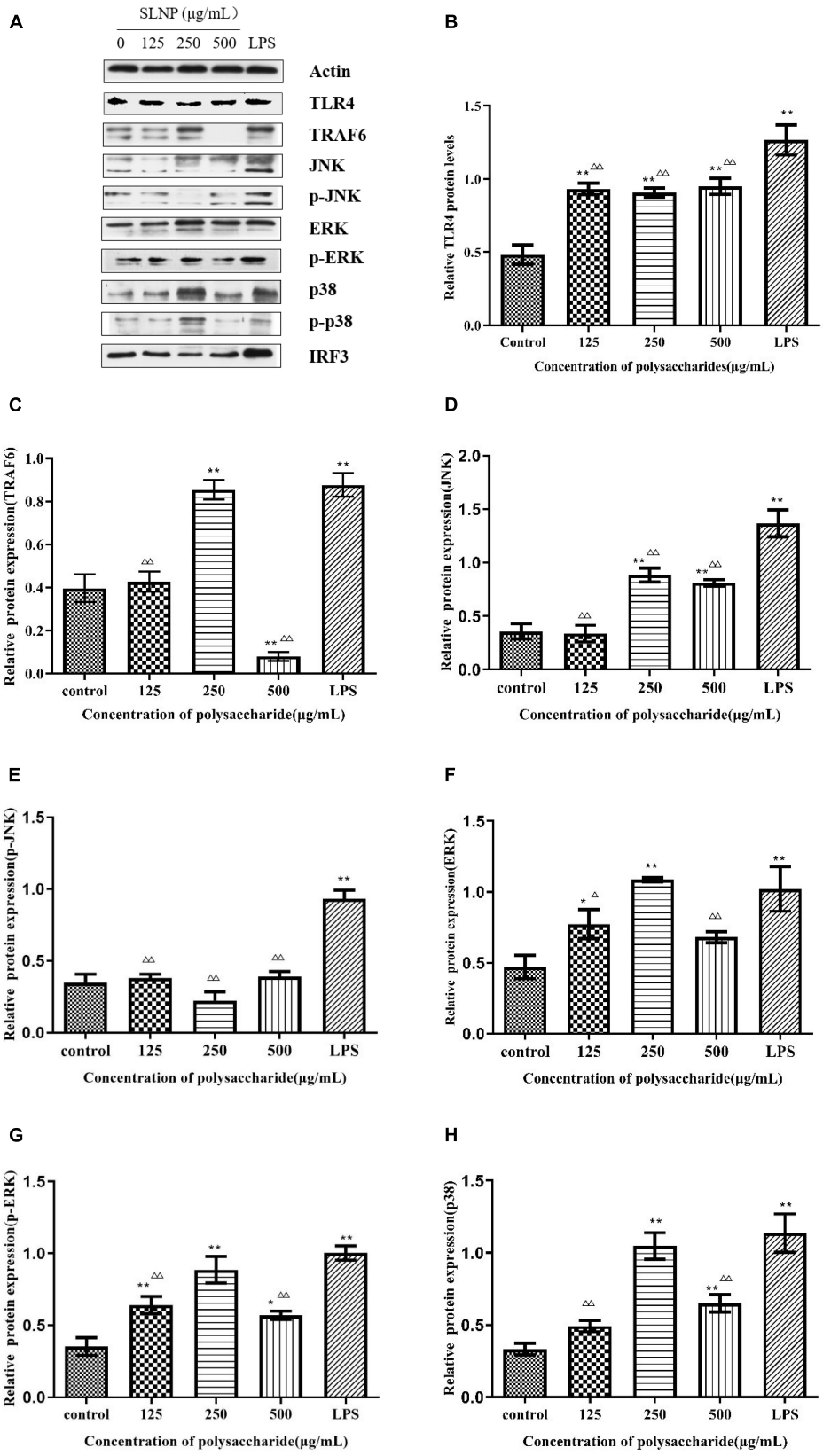

FIGURE 9
(Continued)

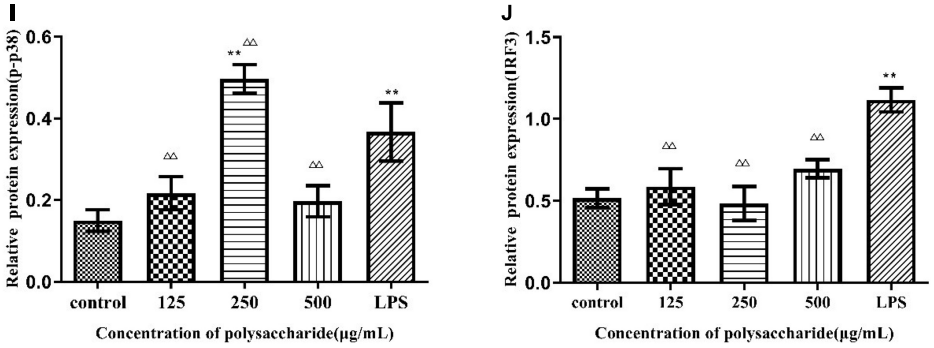

FIGURE 9
Effects of *Sparassis latifolia* neutral polysaccharides SLNP western blot results on protein expression. **(A)**, TLR4 **(B)**, TRAF6 **(C)**, JNK **(D)**, p-JNK **(E)**, ERK **(F)**, p-ERK **(G)**, p38 **(H)**, p-p38 **(I)**, and IRF3 **(J)** in RAW264.7 macrophage. Compared with blank control group, $^{*}p < 0.05$, $^{**}p < 0.01$; Compared with LPS control group, $^{\Delta}p < 0.05$, $^{\Delta\Delta}p < 0.01$.

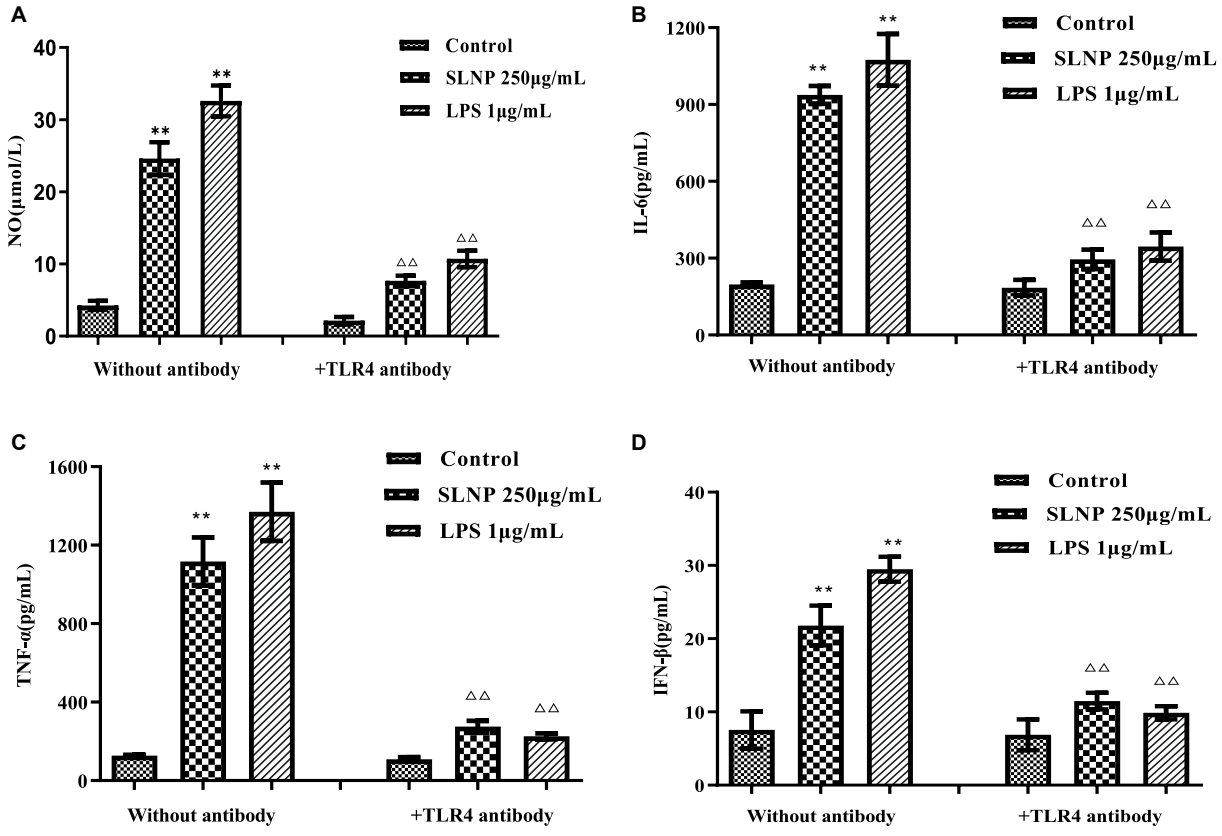

FIGURE 10
Effects of TLR4 antibodies on NO **(A)**, IL-6 **(B)**, TNF-α **(C)**, and IFN-β **(D)** production in RAW264.7 macrophage induced by *Sparassis latifolia* neutral polysaccharides SLNP. Compared with blank control group, $^{*}p < 0.05$, $^{**}p < 0.01$; Compared with LPS control group, $^{\Delta}p < 0.05$, $^{\Delta\Delta}p < 0.01$.

when the concentration reaches 600 μg/mL (50). These results support our study that SLNP not exceeding 1000 μg/mL was able to promote the proliferation of macrophage RAW264.7, indicating that SLNP within 1000 μg/mL don't have cytotoxic effect on RAW264.7 cells. Hence, the dose used in the following studies was based on these results. Moreover, different concentrations of SLNP increased obviously the secretion of NO, IL-6, TNF-α, and IFN-β,

suggesting that SLNP can stimulate macrophages to improve immunity. Similar result is obtained in a previous study of polysaccharides isolated from *Ophiocordyceps sinensis* mycelia (OSP), which shows that OSP significantly improves the immunomodulatory activity in macrophage RAW264.7 cells by promoting the production of TNF-α, IL-6, and IL-1β of macrophage RAW264.7 cells (51). However, when the concentration of polysaccharides exceeds 1000 μg/mL, the phenomenon of inhibition appears. Similar results are obtained in a previous study that a pectic polysaccharide from *Cucurbita moschata Duch* exerts significant suppressive effects on macrophages at 500 μg/mL ($P < 0.05$) (52). The suppression effects of polysaccharides on macrophages may be caused by the facts that high concentrations of polysaccharides may have caused mitochondrial dysfunction, especially the loss of transmembrane mitochondrial potential (53).

The immunomodulatory activity of fungal polysaccharides is inseparable from the immune receptors of macrophages. Polysaccharides bind to immune receptors to activate downstream signal transduction pathways by receptor mediation, transmit signals into cells, initiate immune responses, and promote downstream cytokine secretion (54). TLR4 is a pattern recognition receptor and usually expresses in immune cells including macrophages. The TLR4 signaling pathway is normally regarded to play a vital role in the activation of immune cells (55). Previous studies have shown that TLR4 is a key and undisputed target point of polysaccharides for macrophages, such as *Sarcodon aspratus* polysaccharide (49), *Coriolus versicolor* polysaccharide (56), *Polyporus umbellatus* polysaccharides (57). In the present study, SLNP could promote the mRNA and protein levels of receptor TLR4, and TLR4 antibody blocked the effect of SLNP to stimulate macrophages to secrete NO, IL-6, TNF-α, and IFN-β, which shows that TLR4 is one of the immune receptors of SLNP and involved in the SLNP-mediated activation of macrophages.

TLR4 mediates the secretion of TNF-α and IL-6 through the MyD88 signaling pathway (58). TLR4 can activate two different signaling networks, the MyD88-dependent and MyD88-independent signaling pathways (59). Once antigen is recognized by TLR4, the activated TLR4 recruit adapter protein MyD88 to induce the subsequent response. MyD88-dependent signaling pathways can activate MAPK/NF-κB and thus cause the secretion of cytokines (60). Specifically, the activated TLR4 can promote the phosphorylation of interleukin-1 receptor-related kinase (IRAK-1) to activate TRAF6 (61). Further, the MAKPs family (including JNK, ERK, and p38) is activated to produce phosphorylation and promote the secretion of downstream related immune cytokines (62). In this study, SLNP could promote TLR4 expression, upregulated the mRNA expression of TRAF6, IRF3, JNK, ERK and p38, the protein expression of TRAF6, IRF3, p-JNK, p-ERK, and p-p38, which was proved by the study of JCH-1, a purified polysaccharide isolated from *Isaria cicadae Miquel*. JCH-1 could promote TLR4 expression and up-regulated ERK, JNK, p38 phosphorylation, which indicated that JCH-1 activated RAW264.7 cells through TLR4-MAPK signaling pathway (59). These results imply that SLNP can promote the secretion and expression of various immune cells in the nucleus, such as TNF-α, IL-6, etc., by activating MyD88-dependent signaling pathways *via* TLR4, prompting the activation of TRAF6 to further activate the three target points of JNK, ERK and p38 in the MAPK signaling pathway. In addition, TRIF, another adaptor molecule of TLR4, initiates MyD88-independent signaling pathways resulting in the delayed activation of NFκB. TRIF also phosphorylate IRF3 resulting in the expression of IFN-β (63). Our results indicate that SLNP binding to TLR4 receptor can also signal through MyD88-independent pathways to activate IRF3 and catalyze the expression of IFN-β .

Conclusion

After decolorization and impurity removal by HZ-830 macroporous resin and DEAE-52 separation, the *S. latifolia* polysaccharide was purified by Sepharose CL-6B to obtain the SLNP with the relative Mw of 3.2 Da× 10^5 Da. SLNP was a pyran polysaccharide composed of glucose and galactose. SLNP showed a single symmetrical peak, with an excellent separation effect, high purity, and homogeneity. SLNP could promote the proliferation of RAW264.7 macrophages, which further induced the increased concentration of NO, TNF-α, IL-6, and IFN-β. However, the TLR4 antibody could inhibit significantly the secretion of NO, IL-6, TNF-α, and IFN-β. What's more, SLNP increased remarkably the mRNA and protein levels of TLR4 receptor and the relative expression of mRNA and protein of the signal transduction pathway-related genes TRAF6, IRF3, JNK, ERK, p38, and p38 mediated by the immune receptor TLR4 on the surface of macrophages RAW264.7. These results indicate that TLR4 is the receptor of SLNP and can regulate the immune function of macrophage RAW264.7 through the MyD88-dependent and -independent signaling pathways mediated by the TLR4 receptor.

Data availability statement

The datasets presented in this study can be found in online repositories. The names of the repository/repositories

and accession number(s) can be found in the article/supplementary material.

Author contributions

CF conceived and designed the experiments. ZQ, YZ, and MW coordinated the experiments, contributed to data interpretation, and manuscript writing. JC, MC, SY, YC, and FC participated writing – review and editing. All authors read and approved the final manuscript.

Funding

This work was supported by the Key Research Plan Projects of Shanxi Province (201603D211201), the Collaborative Innovation Center for Enhancing Quality and Efficiency of Loess Plateau Edible Fungi, Scientific and Technological Innovation Team of Edible Mushroom in Shanxi Province (201805D131009), Special Scientific Research Project of Agricultural Valley Construction in Shanxi Province (SXNGJSKYZX201903), and the earmarked fund for Modern Agro-industry Technology Research System in Shanxi Province.

Acknowledgments

We thank the participants in this study for their collaboration and the native English-speaking scientists at Charlesworth Group for editing our manuscript.

Conflict of interest

The authors declare that the research was conducted in the absence of any commercial or financial relationships that could be construed as a potential conflict of interest.

Publisher's note

References

1. Kimura T. Natural products and biological activity of the pharmacologically active cauliflower mushroom *Sparassis latifolia*. *Biomed Res Int.* (2013) 8:501–8. doi: 10.1155/2013/982317

2. Hong KB, Hong SY, Joung EY, Kim BH, Bae SH, Park Y, et al. Hypocholesterolemic effects of the cauliflower culinary-medicinal mushroom, *Sparassis latifolia* (higher basidiomycetes), in diet-induced hypercholesterolemic rats. *Int J Med Mushrooms.* (2015) 17:965–75. doi: 10.1615/intjmedmushrooms.v17.i10.60

3. Yamamoto K, Kimura T. Orally and topically administered *Sparassis latifolia* (Hanabiratake) improved healing of skin wounds in mice with streptozotocin-induced diabetes. *Biosci Biotechnol Biochem.* (2013) 77:1303–5. doi: 10.1271/bbb.121016

4. Hida TH, Kawaminami H, Ishibashi K, Miura NN, Adachi Y, Ohno N. Oral administration of soluble β-glucan preparation from the cauliflower mushroom, *Sparassis latifolia* (higher basidiomycetes) modulated cytokine production in mice. *Int J Med Mushrooms.* (2013) 15:525–38. doi: 10.1615/intjmedmushr.v15.i6.20

5. Harada T, Miura NN, Adachi Y, Nakajima M, Yadomae T, Ohno N. Granulocyte-macrophage colony-stimulating factor (gm-csf) regulates cytokine induction by 1,3-β-d-glucan scg in dba/2 mice in vitro. *J Interf Cytok Res.* (2004) 24:478–89. doi: 10.1089/1079990041689656

6. Harada T, Ohno N. Contribution of dectin-1 and granulocyte macrophage-colony stimulating factor (GM-CSF) to immunomodulating actions of beta-glucan. *Int J Immunopharmacol.* (2008) 8:56–66. doi: 10.1016/j.intimp.2007.12.011

7. Lan MJ, Weng MF, Lin ZY, Wang J, Zhao F, Qiu B. Metabolomic analysis of antimicrobial mechanism of polysaccharides from *Sparassis latifolia* based on HPLC-Q-TOF/MS. *Carbohydr Res.* (2021) 503:108299. doi: 10.1016/j.carres.2021.108299

8. Wang MH, Hao ZQ, Chang MC, Meng JL, Liu JY, Feng CP. Characterization, antioxidant and immunity activities of *Sparassis latifolia* polysaccharides. *J Mycosystema.* (2019) 38:707–16.

9. Evrard D, Szturz P, Tijeras-Raballand A, Astorgues-Xerri L, Abitbol C, Paradis V, et al. Macrophages in the microenvironment of head and neck cancer: potential targets for cancer therapy. *Oral Oncol.* (2019) 88:29–38.

10. Zhang M, Tian X, Wang Y, Wang D, Li W, Chen L, et al. Immunomodulating activity of the polysaccharide TLH-3 from *Tricholoma lobayense* in RAW264.7 macrophages. *Int J Biol Macromol.* (2018) 107:2679–85.

11. Gao ZZ, Liu KH, Tian WJ, Wang HC, Liu ZG, Li YY, et al. Effects of selenizing angelica polysaccharide and selenizing garlic polysaccharide on immune function of murine peritoneal macrophage. *Int Immunopharmacol.* (2015) 27:104–9. doi: 10.1016/j.intimp.2015.04.052

12. Fang Q, Wang JF, Zha XQ, Cui SH, Cao L, Luo JP. Immunomodulatory activity on macrophage of a purified polysaccharide extracted from *Laminaria japonica*. *Carbohydr Polym.* (2015) 134:66–73. doi: 10.1016/j.carbpol.2015.07.070

13. Li M, Yan YX, Yu QT, Deng Y, Wu DT, Wang Y, et al. Comparison of immunomodulatory effects of fresh garlic and black garlic polysaccharides on RAW264.7 macrophages. *J Food Sci.* (2017) 82:765–71. doi: 10.1111/1750-3841.13589

14. Xie SZ, Hao R, Zha XQ, Pan LH, Liu J, Luo JP. Polysaccharide of *Dendrobium huoshanense* activates macrophages *via* toll-like receptor 4-mediated signaling pathways. *Carbohydr Polym.* (2016) 146:292–300. doi: 10.1016/j.carbpol.2016.03.059

15. Fang WS, Bi DC, Zheng RJ, Cai N, Xu H, Zhou R, et al. Identification and activation of TLR4-mediated signaling pathways by alginate-derived guluronate oligosaccharide in RAW264.7 macrophages. *Sci Rep.* (2017) 7:1663. doi: 10.1038/s41598-017-01868-0

16. Zhou L, Liu Z, Wang Z, Yu S, Long T, Zhou X, et al. *Astragalus* polysaccharides exerts immunomodulatory effects *via* TLR4-mediated MyD88-dependent signaling pathway in vitro and in vivo. *Sci Rep.* (2017) 7:44822. doi: 10.1038/srep44822

17. Huang YP, He TB, Cuan XD, Wang XJ, Hu JM, Sheng J. 1,4-β-d-Glucomannan from *Dendrobium officinale* activates NF-κB *via* TLR4 to regulate the immune response. *Molecules.* (2018) 23:2658.

18. Tian H, Liu ZJ, Pu YW, Bao Y. Immunomodulatory effects exerted by *Poria cocos* polysaccharides *via* TLR4/TRAF6/NF-kappaB signaling in vitro and in vivo. *Biomed Pharmacother.* (2019) 112:108709. doi: 10.1016/j.biopha.2019.108709

19. Hsu HY, Hua KF, Lin CC, Lin CH, Hsu J, Wong CH. Extract of Reishi polysaccharides induces cytokine expression *via* TLR4-modulated protein kinase signaling pathways. *J Immunol.* (2004) 173:5989–5899. doi: 10.4049/jimmunol.173.10.5989

20. Wang YQ, Mao JB, Zhou MQ, Jin YW, Lou CH, Dong Y, et al. Polysaccharide from *Phellinus igniarius* activates TLR4-mediated signaling pathways in macrophages and shows immune adjuvant activity in mice. *Int J Biol Macromol.* (2019) 123:157–66. doi: 10.1016/j.ijbiomac.2018.11.066

21. Kim SY, Song HJ, Lee YY, Cho KH, Roh YK. Biomedical issues of dietary fiber β-glucan. *J Korean Med Sci.* (2006) 21:781–9.

22. Park MJ, Ryu HS, Kim JS, Lee HK, Kang JS, Yun J, et al. *Platycodon grandiflorum* polysaccharide induces dendritic cell maturation *via* TLR4 signaling. *Food Chem Toxicol.* (2014) 72:212–20. doi: 10.1016/j.fct.2014.07.011

23. Kim HS, Shin BR, Lee HK, Kim YJ, Park MJ, Kim SY, et al. A polysaccharide isolated from *Pueraria lobata* enhances maturation of murine dendritic cells. *Int J Biol Macromol.* (2013) 52:184–91. doi: 10.1016/j.ijbiomac.2012.09.011

24. Zhang JJ, Song ZT, Li Y, Zhang SJ, Bao JH, Wang HL, et al. Structural analysis and biological effects of a neutral polysaccharide from the fruits of *Rosa laevigata*. *Carbohydr Polym.* (2021) 265:118080. doi: 10.1016/j.carbpol.2021.118080

25. Liu D, Wang SY, Bao YL, Zheng H, Wang GN, Sun Y, et al. Extraction, purification and structural characterization of polysaccharides from *Apocynum venetum* L. roots with anti-inflammatory activity. *Process Biochem.* (2022) 121:100–12.

26. Ma XK, She X, Peterson EC, Wang YZ, Zheng P, Ma HY, et al. A newly characterized exopolysaccharide from *Sanghuangporus sanghuang*. *J Microbiol.* (2019) 57:812–20. doi: 10.1007/s12275-019-9036-4

27. Du YQ, Liu Y, Wang JH. Polysaccharides from *Umbilicaria esculenta* cultivated in Huangshan Mountain and immunomodulatory activity. *Int J Biol Macromol.* (2015) 72:1272–6. doi: 10.1016/j.ijbiomac.2014.09.057

28. Niu JF, Wang SP, Wang BL, Chen LJ, Zhao GM, Liu S, et al. Structure and anti-tumor activity of a polysaccharide from *Bletilla ochracea* Schltr. *Int J Biol Macromol.* (2020) 154:1548–55. doi: 10.1016/j.ijbiomac.2019.11.039

29. Xia L, Ji D, Zhu MX, Chen DF, Lu Y. *Juniperus pingii* var. wilsonii acidic polysaccharide: extraction, characterization and anticomplement activity. *Carbohyd Polym.* (2020) 231:115728. doi: 10.1016/j.carbpol.2019.115728

30. Zhang MT, Yan MX, Yang JQ, Li FF, Wang YR, Feng KY, et al. Structural characterization of a polysaccharide from *Trametes sanguinea* Lloyd with immune-enhancing activity *via* activation of TLR4. *Int J Biol Macromol.* (2022) 206:1026–38. doi: 10.1016/j.ijbiomac.2022.03.072

31. Song JX, Wu Y, Ma XJ, Feng LJ, Wang ZJ, Jiang GQ, et al. Structural characterization and α-glycosidase inhibitory activity of a novel polysaccharide fraction from *Aconitum coreanum*. *Carbohyd Polym.* (2020) 230:115586. doi: 10.1016/j.carbpol.2019.115586

32. Liu CR, Chen JL, Chen L, Huang XS, Cheung PCK. Immunomodulatory activity of polysaccharide-protein complex from the mushroom sclerotia of *Polyporus rhinocerus* in murine macrophages. *J Agric Food Chem.* (2016) 64:3206–14. doi: 10.1021/acs.jafc.6b00932

33. Fitzpatrick JM, Minogue E, Curham L, Tyrrell H, Gavigan P, Hind W, et al. MyD88-dependent and -independent signalling *via* TLR3 and TLR4 are differentially modulated by Δ^9-tetrahydrocannabinol and cannabidiol in human macrophages. *J Neuroimmunol.* (2020) 343:577217. doi: 10.1016/j.jneuroim.2020.577217

34. Zeng WC, Zhang Z, Jia LR. Antioxidant activity and characterization of antioxidant polysaccharides from pine needle (*Cedrus deodara*). *Carbohydr Polym.* (2014) 108:58–64. doi: 10.1016/j.carbpol.2014.03.022

35. Cao JP, Tang DD, Wang Y, Li X, Hong L, Sun CD. Characteristics and immune-enhancing activity of pectic polysaccharides from sweet cherry (*Prunus avium*). *Food Chem.* (2018) 254:47–54. doi: 10.1016/j.foodchem.2018.01.145

36. Wang LC, Chen LY, Li JS, Di LQ, Wu H. Structural elucidation and immune-enhancing activity of peculiar polysaccharides fractioned from marine clam *Meretrix meretrix* (Linnaeus). *Carbohydr Polym.* (2018) 201:500–13. doi: 10.1016/j.carbpol.2018.08.106

37. Cai HL, Huang XJ, Nie SP, Xie MY, Phillips GO, Cui SW. Study on *Dendrobium officinale* O-acetyl-glucomannan (Dendronan®): part iii–immunomodulatory activity in vitro. *Bioact Carbohydr Diet Fibre.* (2015) 5:99–105.

38. Shen CY, Jiang JG, Li MQ, Zheng CY, Zhu W. Structural characterization and immunomodulatory activity of novel polysaccharides from *Citrus aurantium* Linn. variant amara Engl. *J Funct Foods.* (2017) 35:352–62.

39. Zhang MM, Wang G, Lai FR, Wu H. Structural characterization and immunomodulatory activity of a novel polysaccharide from *Lepidium meyenii*. *J Agric Food Chem.* (2016) 64:1921–31. doi: 10.1021/acs.jafc.5b05610

40. Du J, Li JJ, Zhu JH, Huang CH, Bi SX, Song LY, et al. Structural characterization and immunomodulatory activity of a novel polysaccharide from *Ficus carica*. *Food Funct.* (2018) 9:3930–43. doi: 10.1039/c8fo00603b

41. Song QQ, Jiang L, Yang XQ, Huang LX, Yu Y, Yu Q, et al. Physicochemical and functional properties of a water-soluble polysaccharide extracted from mung bean (*Vigna radiate* L.) and its antioxidant activity. *Int J Biol Macromol.* (2019) 138:874–80. doi: 10.1016/j.ijbiomac.2019.07.167

42. Feng YQ, Juliet IC, Wen CT, Duan YQ, Zhou J, He YQ, et al. Effects of multi-mode divergent ultrasound pretreatment on the physicochemical and functional properties of polysaccharides from *Sagittaria sagittifolia* L. *Food Biosci.* (2021) 42:101145.

43. Ghoreschi K, Jesson MI, Li X, Lee JL, Ghosh S, Alsup JW, et al. Modulation of innate and adaptive immune responses by tofacitinib (CP-690,550). *J Immunol.* (2011) 186:4234–43.

44. Zhu EF, Gai SA, Opel CF, Kwan BH, Surana R, Mihm MC, et al. Synergistic innate and adaptive immune response to combination immunotherapy with anti-tumor antigen antibodies and extended serum half-life IL-2. *Cancer Cell.* (2015) 27:489–501. doi: 10.1016/j.ccell.2015.03.004

45. Janeway CA, Medzhitov R. Innate immune recognition. *Ann Rev Immunol.* (2002) 20:197–216.

46. Wang YF, Tian Q, Shao JJ, Shu X, Jia JX, Ren XJ, et al. Macrophage immunomodulatory activity of the polysaccharide isolated from *Collybia radicata* mushroom. *Int J Biol Macromol.* (2018) 108:300–6. doi: 10.1016/j.ijbiomac.2017.12.025

47. Liu QM, Xu SS, Li L, Pan TM, Shi CL, Liu H, et al. In vitro and in vivo immunomodulatory activity of sulfated polysaccharide from *Porphyra haitanensis*. *Carbohydr Polym.* (2017) 165:189–96.

48. Kuang MT, Xu JY, Li JY, Yang L, Hou B, Zhao Q, et al. Purification, structural characterization and immunomodulatory activities of a polysaccharide from the fruiting body of *Morchella sextelata*. *Int J Biol Macromol.* (2022) 213:394–403. doi: 10.1016/j.ijbiomac.2022.05.096

49. Wang DD, Pan WJ, Mehmood S, Cheng XD, Chen Y. Polysaccharide isolated from *Sarcodon aspratus* induces RAW264.7 activity *via* TLR4-mediated NF-κB and MAPK signaling pathways. *Int J Biol Macromol.* (2018) 120:1039–47. doi: 10.1016/j.ijbiomac.2018.08.147

50. Li YL, Li XJ, Chu Q, Jia RY, Chen W, Wang YX, et al. *Russula alutacea* Fr. polysaccharide ameliorates inflammation in both RAW264.7 and zebrafish (Danio rerio) larvae. *Int J Biol Macromol.* (2020) 145:740–9. doi: 10.1016/j.ijbiomac.2019.12.218

51. Liu Y, Li QZ, Li LDJ, Zhou XW. Immunostimulatory effects of the intracellular polysaccharides isolated from liquid culture of *Ophiocordyceps sinensis* (Ascomycetes) on RAW264.7 cells *via* the MAPK and PI3K/Akt signaling pathways. *J Ethnopharmacol.* (2021) 275:114130. doi: 10.1016/j.jep.2021.114130

52. Huang LL, Zhao J, Wei YL, Yu GY, Li F, Li QH. Structural characterization and mechanisms of macrophage immunomodulatory activity of a pectic polysaccharide from *Cucurbita moschata* Duch. *Carbohydr Polym.* (2021) 269:118288. doi: 10.1016/j.carbpol.2021.118288

53. Xiong L, Ouyang KH, Jiang Y, Yang ZW, Hu WB, Chen H, et al. Chemical composition of *Cyclocarya paliurus* polysaccharide and inflammatory effects in lipopolysaccharide-stimulated RAW264.7 macrophage. *Int J Biol Macromol.* (2018) 107:1898–907. doi: 10.1016/j.ijbiomac.2017.10.055

54. Hosseini AM, Majidi J, Baradaran B, Yousefi M. Toll-like receptors in the pathogenesis of autoimmune diseases. *Adv Pharm Bull.* (2015) 5:605–14.

55. Gay NJ, Symmons MF, Gangloff M, Bryant CE. Assembly and localization of Toll-like receptor signalling complexes. *Nat Rev Immunol.* (2014) 14:546–58.

56. Price LA, Wenner CA, Sloper DT, Slaton JW, Novack JP. Role for toll-like receptor 4 in TNF-α secretion by murine macrophages in response to polysaccharide Krestin, a *Trametes versicolor* mushroom extract. *Fitoterapia.* (2010) 81:914–9. doi: 10.1016/j.fitote.2010.06.002

57. Li XQ, Xu W. TLR4-mediated activation of macrophages by the polysaccharide fraction from *Polyporus umbellatus* (pers.) fries. *J Ethnopharmacol.* (2010) 3:168–76. doi: 10.1016/j.jep.2010.06.028

58. Park HJ, Hong JH, Kwon HJ, Kim Y, Lee KH, Kim JB, et al. TLR4-mediated activation of mouse macrophages by Korean mistletoe lectin-C (KML-C). *Biochem Biophys Res Commun.* (2010) 396:721–5. doi: 10.1016/j.bbrc.2010.04.169

59. Xu ZC, Lin RY, Hou X, Wu J, Zhao WB, Ma HH, et al. Immunomodulatory mechanism of a purified polysaccharide isolated from *Isaria cicadae* Miquel on RAW264.7 cells *via* activating TLR4-MAPK-NF-κB signaling pathway. *Int J Biol Macromol.* (2020) 164:4329–38. doi: 10.1016/j.ijbiomac.2020.09.035

60. Qiao Y, Giannopoulou EG, Chan CH, Park SH, Gong SC, Chen J, et al. Activation of inflammatory cytokine genes by interferon-γ-induced chromatin remodeling and toll-like receptor signaling. *Immunity.* (2013) 39:454–69. doi: 10.1016/j.immuni.2013.08.009

61. Dong W, Liu YL, Peng JH, Chen L, Zou TT, Xiao HZ, et al. The IRAK-1-BCL10-MALT1-TRAF6-TAK1 cascade mediates signaling to NF-κB from toll-like receptor 4. *J Biol Chem.* (2006) 281:26029–40. doi: 10.1074/jbc.M513057200

62. Gupta PK, Rajan MGR, Kulkarni S. Activation of murine macrophages by G1-4A, a polysaccharide from *Tinospora cordifolia*, in TLR4/MyD88 dependent manner. *Int Immunopharmacol.* (2017) 50:168–77. doi: 10.1016/j.intimp.2017.06.025

63. Lee JY, Lowell CA, Lemay DG, Youn HS, Rhee SH, Sohn KH, et al. The regulation of the expression of inducible nitric oxide synthase by Src-family tyrosine kinases mediated through MyD88-independent signaling pathways of toll-like receptor 4. *Biochem Pharmacol.* (2005) 70:1231–40. doi: 10.1016/j.bcp.2005.07.020